

Physical parameter study of eight W Ursae Majoris-type contact binaries in NGC 188

Xiaodian Chen^{1,2}, Licai Deng², Richard de Grijs^{1,3}, Xiaobin Zhang², Yu Xin², Kun Wang^{2,4}, Changqing Luo², Zhengzhou Yan^{2,4}, Jianfeng Tian², Jinjiang Sun⁵, Qili Liu⁵, Qiang Zhou⁵, and Zhiquan Luo⁴

ABSTRACT

We used the newly commissioned 50 cm Binocular Network (50BiN) telescope at Qinghai Station of Purple Mountain Observatory (Chinese Academy of Sciences) to observe the old open cluster NGC 188 in V and R as part of a search for variable objects. Our time-series data span a total of 36 days. Radial-velocity and proper-motion selection resulted in a sample of 532 genuine cluster members. Isochrone fitting was applied to the cleaned cluster sequence, yielding a distance modulus of $(m - M)_V^0 = 11.35 \pm 0.10$ mag and a total foreground reddening of $E(V - R) = 0.062 \pm 0.002$ mag. Light-curve solutions were obtained for eight W Ursae Majoris eclipsing-binary systems (W UMas) and their orbital parameters were estimated. Using the latter parameters, we estimate a distance to the W UMas which is independent of the host cluster's physical properties. Based on combined fits to six of the W UMas (EP Cep, EQ Cep, ES Cep, V369 Cep, and—for the first time—V370 Cep and V782 Cep), we obtain an average distance modulus of $(m - M)_V^0 = 11.31 \pm 0.08$ mag, which is comparable with that resulting from our isochrone fits. These six W UMas exhibit an obvious period–luminosity relation. We derive more accurate physical parameters for the W UMa systems and discuss their initial masses and ages. The former show that these W UMa systems have likely undergone angular-momentum evolution within a convective envelope (W-type evolution). The ages of the W UMa systems agree well with the cluster's age.

¹Kavli Institute for Astronomy & Astrophysics and Department of Astronomy, Peking University Yi He Yuan Lu 5, Hai Dian District, Beijing 100871, China; chenxiaodian1989@163.com, grijs@pku.edu.cn

²Key Laboratory for Optical Astronomy, National Astronomical Observatories, Chinese Academy of Sciences, 20A Datun Road, Chaoyang District, Beijing 100012, China

³International Space Science Institute–Beijing, 1 Nanertiao, Zhongguancun, Hai Dian District, Beijing 100190, China

⁴School of Physics & Electronic Information, China West Normal University, Nanchong 637002, China

⁵Purple Mountain Observatory, Chinese Academy of Sciences, Nanjing 210008, China

Subject headings: methods: data analysis – Galaxy: open clusters and associations: individual (NGC 188, Berkeley 39) – stars: binaries: eclipsing – stars: distances

1. Introduction

W Ursae Majoris (W UMa) variables are low-mass, so-called “overcontact” binary systems, where the Roche lobes of both stellar components are filled. W UMas share a common convective envelope. Both components are characterized by rapid rotation, with periods ranging from $P = 0.2$ d to $P = 1.0$ d. It is straightforward to obtain complete and high-quality W UMa light curves in a few nights of observing time on small to moderate-sized telescopes.

Since W UMas are very common in both old open clusters (OCs) and the Galactic field, they have significant potential as distance indicators. Approximately 0.1% of the F-, G-, and K-type dwarfs in the solar neighborhood are W UMas (Duerbeck 1984), while in OCs their frequency may be as high as $\sim 0.4\%$ (Rucinski 1994). Although the occurrence frequency of main-sequence contact binaries in old globular clusters is low, the frequency of “blue straggler”-type contact binary systems is two to three times higher there than that in OCs (Rucinski 2000). W UMas can reveal the evolutionary history of their host cluster, since they are thought to result from dynamical interactions in the cluster. Alternatively, these systems may represent a possible final evolutionary phase of primordial binary systems, once these binaries have lost most of their angular momentum. Since W UMas are more than 4 mag fainter than Cepheids or RR Lyrae variables, studies of W UMa distances have only been undertaken for just a few decades. Rucinski & Duerbeck (1997) used W UMas as distance tracers for 400 objects from the Optical Gravitational Lensing Experiment (OGLE) variable-star catalog.

If a reliable (orbital) period–luminosity (PL) relation can be established for W UMa systems, they could potentially play a similarly important role as Cepheids in measuring the distances to old structures in the Milky Way, including those traced by old OCs and the Galactic bulge. Although distances based on individual W UMas are not as accurate as those resulting from Cepheid analysis, their large numbers could potentially overcome this disadvantage. Clusters represent good stellar samples to study distances, because their distances can be estimated in a number of independent ways (e.g., Chen et al. 2015). In our modern understanding, these systems are most likely formed through either nuclear evolution of the most massive component in the detached phase (A subtype) or angular-momentum evolution of the two component stars within a convective envelope (W subtype)

(Hilditch et al. 1988; Yıldız & Doğan 2013). Yıldız (2014) provided a method to calculate the typical evolution timescales of W UMa systems. Armed with accurate distances, significantly improved physical parameters (such as masses and luminosities) can be determined. In turn, such W UMa systems can then be used to constrain the evolution of W UMa systems in general.

NGC 188 is an old OC at a distance of ~ 2 kpc. It contains a large number of W UMa variables. Seven W UMas near its center were first found by Hoffmeister (1964) and Kaluzny & Shara (1987). Zhang et al. (2002, 2004) undertook a detailed survey covering 1 deg^2 around the cluster center and found 16 W UMas. Branly et al. (1996) calculated light-curve solutions for five central W UMas using the Wilson–Devinney (W–D) code and discussed the W UMa distance in relation to the cluster distance. Liu et al. (2011) obtained orbital solutions for EQ Cep, ER Cep, and V371 Cep, while Zhu et al. (2014) published similar results for three additional W UMas, i.e., EP Cep, ES Cep, and V369 Cep.

In this paper, we study all eight previously identified NGC 188 W UMas based on high-cadence observations obtained over a continuous period of more than two months, resulting in accurate, self-consistent, and homogeneous magnitudes and a well-determined average distance, relying on up to 3000 data points for a single W UMa system. We also establish a physical relationship between these eight variables and their host cluster, NGC 188, based on proper motions, radial velocities, and features in the color–magnitude diagram (CMD). Although Cepheid variables are among the most useful objects to establish the distance ladder, the small number of Cepheids in our Galaxy introduces relatively large statistical errors, while their disparate distances introduce comparably large systematic errors in distance modulus, reddening (An et al. 2007), and metallicity (Sandage et al. 2008). Compared with bright O- and B-type Cepheids, faint W UMa dwarfs are much more plentiful. Our aim is to obtain more accurate cluster distances than available to date based on our new W UMa observations and, consequently, improve the corresponding PL relation. At the same time, an important secondary goal is to obtain significantly improved W UMa stellar parameters, thus allowing us to better constrain the evolution of our cluster W UMa systems as a population.

In Section 2, we discuss our observations and the calibration of both the NGC 188 data and the W UMa properties used in this study. The light-curve results, as well as the results from CMD fitting, proper-motion, and radial-velocity selection, and our distance analysis, are covered in Section 3. We discuss the properties of our eight sample W UMas, as well as the feasibility of using W UMas as distance indicators, e.g., based on their period–luminosity–color (PLC) or PL relations, in Section 4. In Section 5, we summarize our main conclusions.

2. Observations and data reduction

We observed the OC NGC 188 for a total of 36 nights during two separate periods—2014 September 28 to 2014 October 7, and 2016 January 13 to 2016 March 10—using the 50 cm Binocular Network telescope (50BiN; Deng et al. 2013) at the Qinghai Station of Purple Mountain Observatory (Chinese Academy of Sciences). The time-series light-curve observations in the Johnson V and R bands were obtained simultaneously using two Andor $2k \times 2k$ CCDs. The telescope’s field of view is 20×20 arcmin², which is adequate for covering the central region of NGC 188. Details of the observations are included in Table 1. Preliminary processing (bias and dark-frame subtraction, as well as flat-field corrections) of the CCD frames was performed with the standard CCDPROC tasks in IRAF. Point-spread-function photometry was extracted using the DAOPHOT II package. Based on a comparison with the NGC 188 $UBVRI$ photometric catalog of Sarajedini et al. (1999), we calibrated the stellar fluxes and atmospheric absorption for a data set spanning 7 days (2014 October 1–7). The transfer function is given by

$$\begin{aligned} V_0 &= V + a \times (V - R) + b; \\ R_0 &= R + c \times (V - R) + d, \end{aligned} \tag{1}$$

where V and R are the instrumental magnitudes, while V_0 and R_0 are the calibrated magnitudes. The highest-quality VR data were selected for our color–magnitude analysis, while time-series data were extracted to find and study variable stars.

3. Results

3.1. Membership and Color–Magnitude Diagram

Our initial data set contained 914 stars with photometry in both the V and R filters, and with photometric errors $\sigma_V \leq 0.1$ mag for $V \leq 18$ mag. We further refined the data set, aiming to only select genuine cluster members, using proper-motion and radial-velocity selection. The proper-motion data were obtained from Platais et al. (2003). Their data base contains proper motions and positions for 7812 objects down to $V = 21$ mag in a 0.75 deg² area around NGC 188. Of our 914 initial sample objects, proper motions measurements were available for 910. The locus dominated by the cluster members in the proper-motion distribution is obvious: see Fig. 1. First, we estimated the time average and standard deviation for all stars in the distribution so as to exclude high proper-motion stars, adopting a 1.5σ selection cut (see Fig. 1). To exclude stars with very large proper motions and, thus, to only retain the most probable cluster members, this process was repeated twice (where

the distribution’s σ was redetermined after the first selection cut), resulting in an average cluster proper motion of $(\mu_\alpha, \mu_\delta) = (-5.2 \pm 0.6, -0.3 \pm 0.6)$ mas yr⁻¹. Of the 910 sample stars with measured proper motions, 558 are located within the (final) 1.5σ distribution and they are thus considered cluster members for the purposes of this paper. Figure 1 shows the NGC 188 proper-motion distribution; six W UMas (red triangles) satisfy the selection criteria adopted and are thus most likely NGC 188 W UMas. Two additional W UMas, i.e., V₃ and V₇ (green triangles), are located within the 3σ distribution; they are considered possible OC W UMas.

The average radial-velocity measurements were taken from Geller et al. (2008). Their sample includes 1046 stars in a 1 deg² field centered on NGC 188. Radial velocities are known for 433 of the 914 stars in our initial sample. To exclude stars with very large radial velocities, we applied a three-step¹ selection procedure to all of these 433 stars, adopting (new) 3σ selection cuts each time, and obtained $v_{\text{RV}} = -42.32 \pm 0.90$ km s⁻¹ for the cluster. A total of 93 stars were excluded from our final sample, leaving 340 genuine cluster members.

Figure 2 shows the cluster members’ $V, (V - R)$ CMD. After radial-velocity and proper-motion selection, the cluster members delineate a clear main sequence, also exhibiting some blue stragglers, as well as a discernible binary sequence. This old OC has a high binary frequency of approximately 23% (Geller & Mathieu 2012). We adopted the Dartmouth stellar isochrones (Dotter et al. 2008) for further analysis of the cluster’s CMD, since they seem to best match our VR photometry. The Padova isochrones (Girardi et al. 2000) exhibit a shift in the locus of the red-giant branch, while the Yale isochrones (Yi et al. 2001) cannot be used to match the faint end of the main sequence ($17 \leq V \leq 18$ mag). The red line represents the best-fitting isochrone for an age of 6 Gyr and $[\text{Fe}/\text{H}] = 0.0$ dex. We obtained $E(V - R) = 0.062 \pm 0.002$ mag and $(m - M)_V^0 = 11.35 \pm 0.10$ mag. Since the colors of W UMas do not vary significantly during any given orbital period, we assume $\langle V - R \rangle = \langle V \rangle - \langle R \rangle$. The loci of the eight W UMas, based on averaging our photometry over four periods, are shown as red solid bullets in the CMD, adopting the average maximum magnitudes for each.

3.2. W UMa light-curve solutions

Based on our time-series data, all eight central W UMas were identified and marked V₁–V₇ and V₁₃ (Zhang et al. 2004). We obtained the best-fitting light-curve solutions for eight W UMa systems using the same W–D code. First, we can derive the average temperature T ,

¹A three-step procedure resulted in the most stable number of members in the final sample; a similar result was obtained in two steps based on the tabulated proper motions.

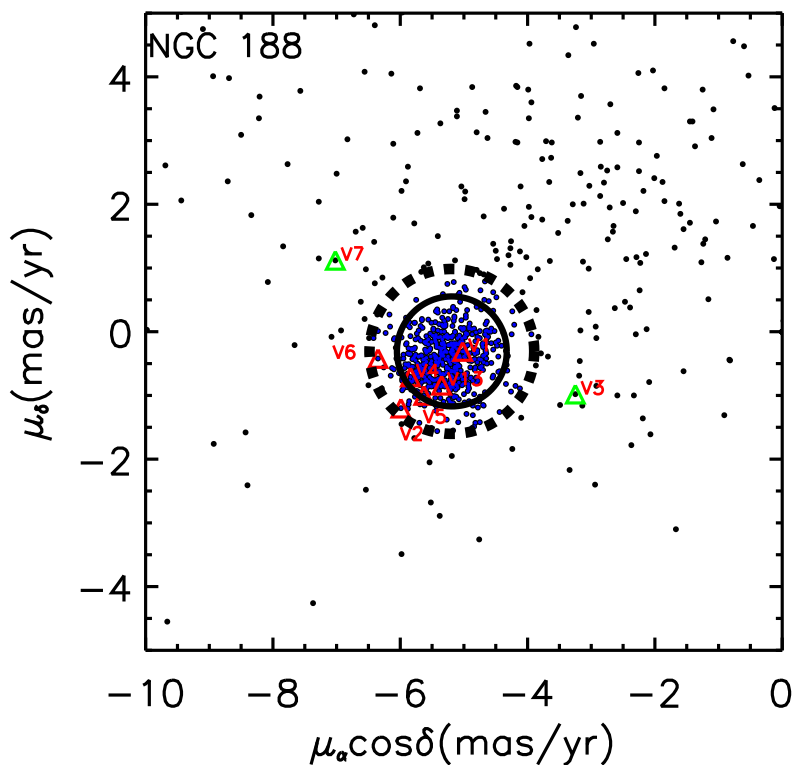


Fig. 1.— Proper-motion distribution of stars in NGC 188 (Platais et al. 2003). The dotted and solid circles represent the 1.5σ and 1σ radii, respectively. The blue dots are stars located within the (final) 1.5σ radius, which are treated as genuine cluster members. The triangles represent the W UMas’ proper motions; red: likely OC W UMas, green: possible OC W UMas, located at $\gtrsim 3\sigma$ from the center of the distribution.

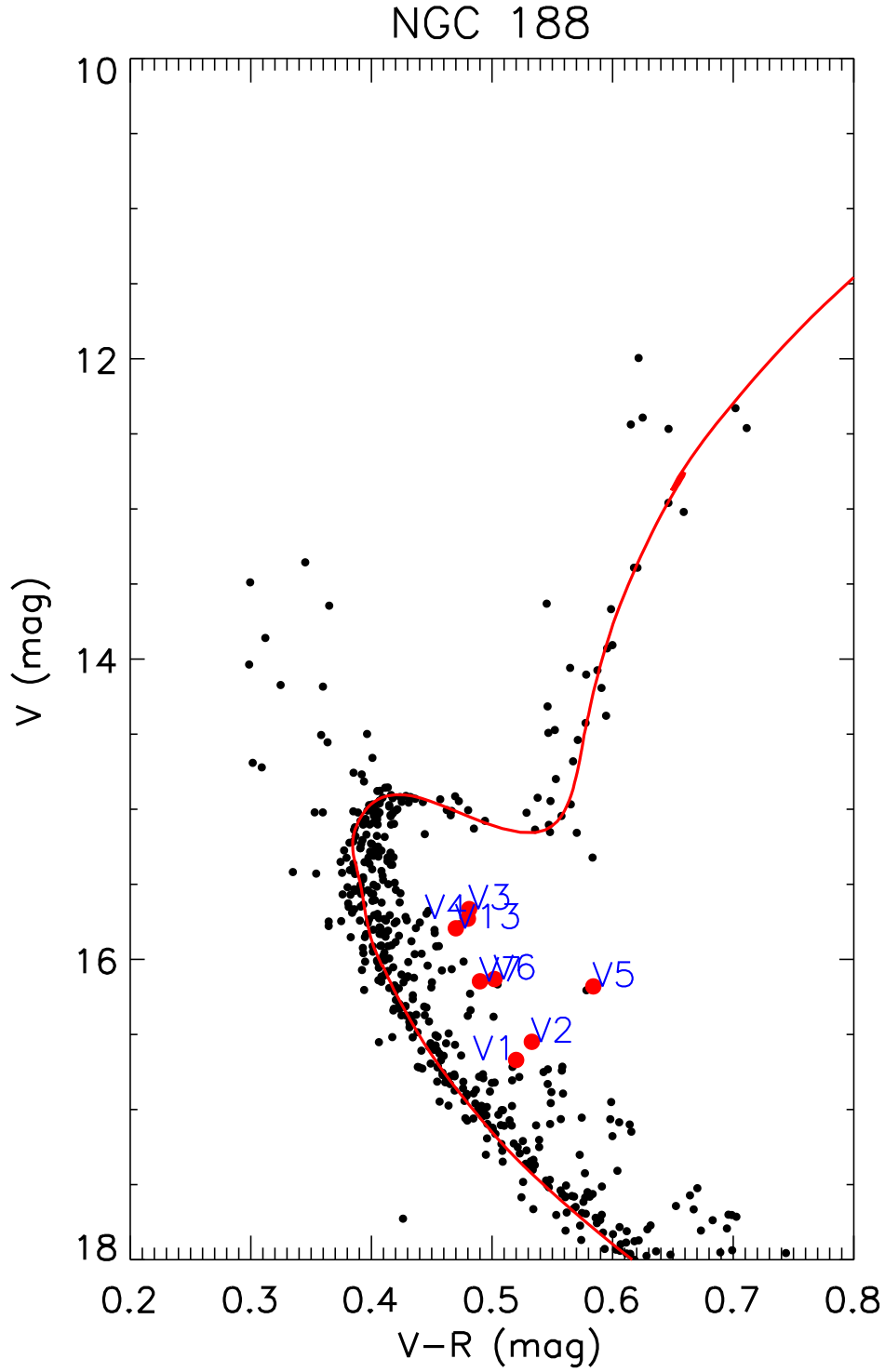


Fig. 2.— Best-fitting isochrone to the CMD of the OC NGC 188. The black dots are the genuine cluster members remaining after radial-velocity and proper-motion selection. The solid red line is the best-fitting isochrone for solar metallicity. The red bullets represent the average $(V - R)$ colors and maximum V magnitudes for the eight cluster W UMas.

from its intrinsic color. A rough estimate can be obtained using $T = 8540/[(B - V)_0 + 0.865]$ K. This is usually sufficient, because its precise value only affects the temperature of the two components, T_1 , T_2 , in the W–D code, while its effect on the other key parameters, including the mass ratio, stellar radii, and inclination, is very small. If one is only interested in deriving orbital parameters, T does not need to be known to very high accuracy. However, W UMa distance determination depends on knowing a system’s color: see Section 3.4. In this paper, our goal is to determine temperature-independent distances to our W UMa sample systems. We therefore need to determine the $(V - R)$ colors more accurately and apply proper reddening corrections, using $E(V - R) = 0.062$ mag (see Section 3.1). This implies that we need to obtain more accurate values for T , which we can derive from interpolation of the theoretical color–temperature catalog of Lejeune et al. (1997). Then, the most important parameter to constrain is the mass ratio, $q = m_2/m_1$, where m_1 and m_2 are the masses of the system’s two components, respectively. The mass ratio can be estimated directly from the radial velocity; q is the inverse of the ratio of the components’ rotational velocities. However, since the eight W UMas have magnitudes around $V = 16$ mag and considering their rapidly changing velocities, sufficient-quality spectra can only be obtained using large-aperture telescopes. In addition, a number of binaries only show a single line in their spectra, so that q cannot be obtained easily. In the latter case, we can test for $q \in [0.1, 10.0]$ and adopt the mass ratio yielding the smallest residual as q (see Fig. 3). We tested this method extensively to ascertain that this is a suitable approach to adequately constrain q ; this method is most effective for W UMa systems seen under higher inclinations.

The relevant gravity-darkening factor required for application of the W–D code is usually set at 0.32 and 1.0 for stars dominated by convective and radiative energy transport, respectively, and the corresponding reflection factors are 0.5 and 1.0. The bolometric limb-darkening coefficient for different filters is given by van Hamme (1993). We also need to adjust T_2 , the components’ (dimensionless) surface potentials, $\Omega_1 = \Omega_2$, the primary star’s luminosity, L_1 , and the orbital inclination, i . Figure 4 shows all observations in phase, with the code’s best-fitting light-curve solutions overplotted. All eight sample W UMas are matched perfectly. Based on assessment of these light curves, our best fits are significantly better than those published previously (Branly et al. 1996; Liu et al. 2011; Zhu et al. 2014), which is largely driven by the much larger number of observational data points per single period (and their very homogeneous nature) used for the fits. Rucinski (1994) used NGC 188 photometry from Kaluzny & Shara (1987), which represented no more than 40 data points for a given period; the scatter associated with their light curves is easily discernible. The photometric quality used by Branly et al. (1996) was better than that of Kaluzny & Shara (1987), at least in the V band (the B -band quality was insufficient for reliable light-curve fits).

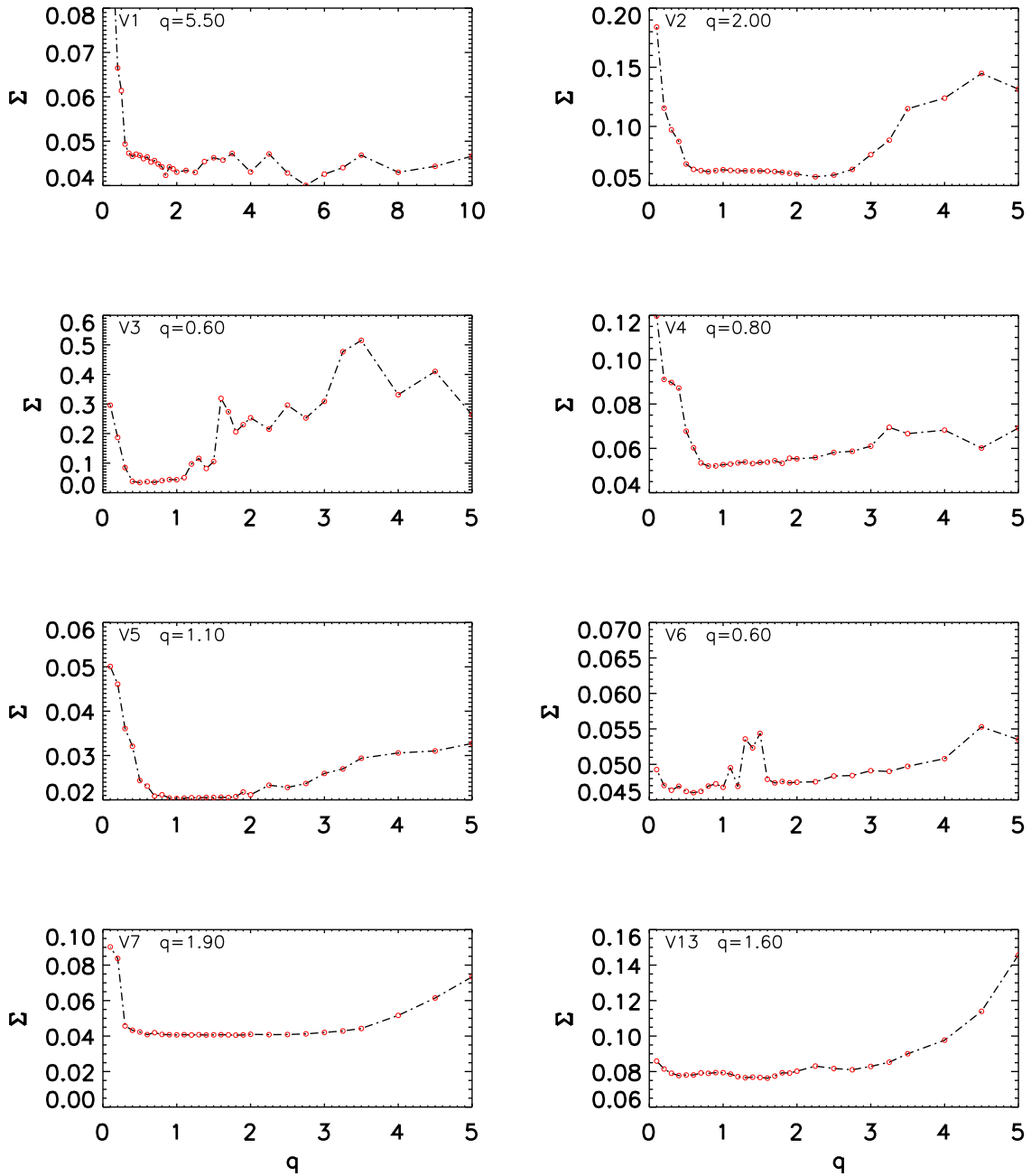


Fig. 3.— Tests to obtain the most appropriate mass ratios, q , i.e., those yielding the smallest residuals.

Table 1: Observation log

Date	Frames (<i>V</i>)	Frames (<i>R</i>)	Date	Frames (<i>V</i>)	Date	Frames (<i>V</i>)
2014 Sep 28	142	205	2016 Jan 25	108	2016 Feb 09	107
2014 Oct 01	219	314	2016 Jan 26	111	2016 Feb 14	100
2014 Oct 02	122	196	2016 Jan 27	112	2016 Feb 17	104
2014 Oct 04	204	336	2016 Jan 28	50	2016 Feb 19	106
2014 Oct 05	209	297	2016 Jan 29	46	2016 Feb 22	96
2014 Oct 07	130	212	2016 Jan 30	50	2016 Feb 24	103
2016 Jan 13	116		2016 Feb 02	112	2016 Feb 25	104
2016 Jan 14	107		2016 Feb 03	95	2016 Feb 27	88
2016 Jan 15	98		2016 Feb 04	91	2016 Feb 28	102
2016 Jan 20	110		2016 Feb 05	96	2016 Feb 29	105
2016 Jan 22	107		2016 Feb 06	102	2016 Mar 05	100
2016 Jan 23	82		2016 Feb 07	101	2016 Mar 07	95

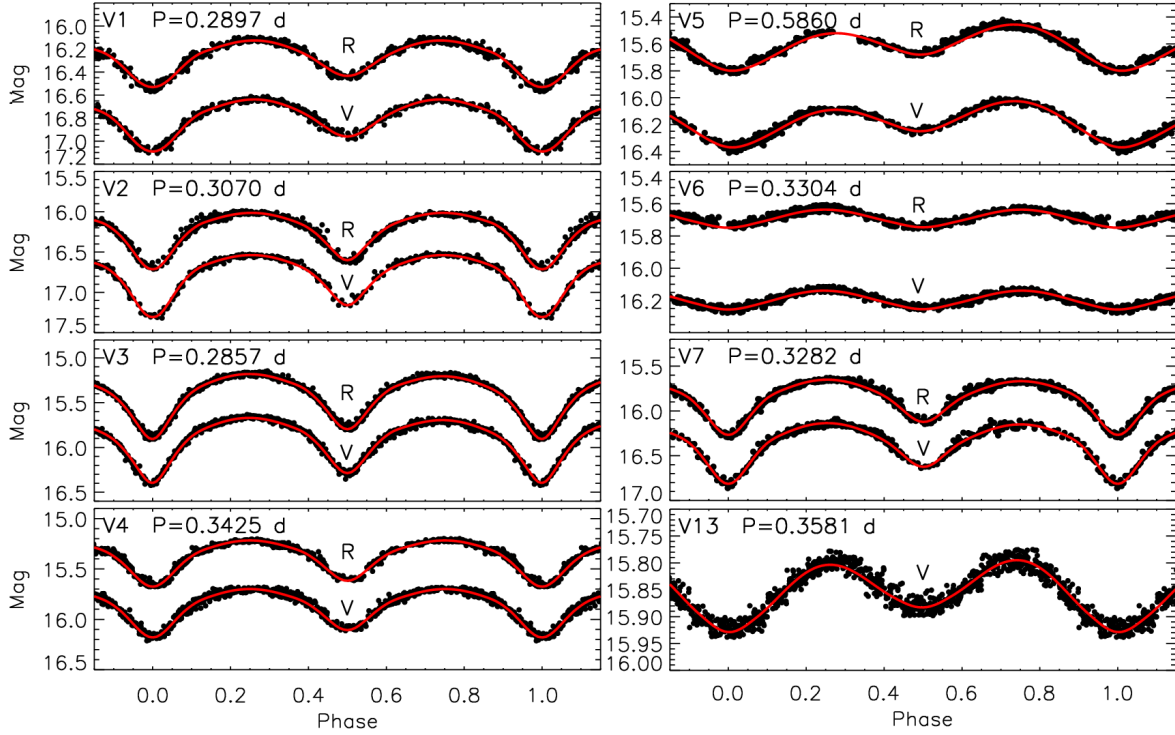


Fig. 4.— Observations and code solutions of the light curves of eight W UMas in NGC 188. The black dots are the observational data, while the solid line is the model solution.

Table 2: Light-curve solutions for the eight W UMa systems in NGC 188.

Parameters	V_1 (EP Cep)	V_2 (EQ Cep)	V_3 (ER Cep)	V_4 (ES Cep)	V_6 (V370 Cep)	V_7 (V369 Cep)	V_5 (V371 Cep)	V_{13} (V782 Cep)
V_{\max}, R_{\max} (mag)	16.670,16.150	16.549,16.016	15.665,15.184	15.729,15.249	16.131,15.629	16.146,15.656	16.046,15.470	15.793
V_{\min}, R_{\min} (mag)	17.084,16.543	17.301,16.731	16.409,15.889	16.140,15.646	16.245,15.748	16.808,16.269	16.390,15.803	15.931
$V_{\text{avg}}, R_{\text{avg}}$ (mag)	16.811,16.286	16.776,16.235	15.887,15.398	15.878,15.393	16.183,15.684	16.344,15.844	16.180,15.596	15.858
T (K)	5182	5083	5458	5465	5313	5396	4862	5526
T_1 (K)	5600	5275	5505	5582	5383	5546	4780	5750
T_2 (K)	5074 ± 17	4975 ± 9	5383 ± 10	5308 ± 14	5175 ± 88	5088 ± 12	4935 ± 33	5370 ± 69
$\Omega_1 = \Omega_2$	9.56 ± 0.03	5.35 ± 0.01	3.09 ± 0.01	3.40 ± 0.02	2.93 ± 0.05	5.01 ± 0.02	3.77 ± 0.01	4.73 ± 0.07
i ($^\circ$)	69.45 ± 0.32	81.40 ± 0.23	79.69 ± 0.15	71.07 ± 0.14	46.62 ± 2.24	74.71 ± 0.18	53.86 ± 0.70	44.14 ± 2.72
$L_{V_1}/(L_{V_1} + L_{V_2})$	0.27 ± 0.01	0.41 ± 0.01	0.66 ± 0.01	0.61 ± 0.01	0.68 ± 0.02	0.47 ± 0.02	0.44 ± 0.02	0.46 ± 0.02
$q = m_2/m_1$	5.41 ± 0.02	2.09 ± 0.01	0.63 ± 0.01	0.78 ± 0.01	0.52 ± 0.02	1.90 ± 0.01	1.06 ± 0.01	1.60 ± 0.03
r_1	0.251 ± 0.002	0.320 ± 0.002	0.424 ± 0.001	0.398 ± 0.003	0.432 ± 0.013	0.334 ± 0.003	0.384 ± 0.003	0.331 ± 0.006
r_2	0.537 ± 0.002	0.449 ± 0.002	0.343 ± 0.001	0.354 ± 0.003	0.318 ± 0.012	0.446 ± 0.003	0.395 ± 0.003	0.415 ± 0.006
$(m - M)_V^0$ (mag)	11.382 ± 0.117	11.280 ± 0.111	10.781 ± 0.093	11.188 ± 0.092	11.294 ± 0.122	11.412 ± 0.095	11.563 ± 0.101	11.314 ± 0.115
θ_1 ($^\circ$)							32.09	23.61
ψ_1 ($^\circ$)							315.28	341.08
$r_{\text{spot},1}$ ($^\circ$)							24.97	18.66
$T_{\text{spot},1}/T$							0.50	0.73
θ_2 ($^\circ$)			79.22				16.39	
ψ_2 ($^\circ$)			232.17				165.10	
$r_{\text{spot},2}$ ($^\circ$)			15.80				25.77	
$T_{\text{spot},2}/T$			0.71				0.68	
Residual σ (mag)	0.040	0.058	0.035	0.050	0.046	0.041	0.021	0.076
Membership	Y	Y	N	Y	Y	Y	Y	Y

3.3. Primary stellar masses

In principle, to determine accurate distances to W UMa systems, we must have access to two absolute measurements. Since we only have relative photometric data for our eight NGC 188 W UMas, we need to indirectly obtain absolute measurements using an approximate method. Fortunately, W UMas are similar to F-, G-, and K-type main-sequence stars. For these stellar types, semi-observational, empirical, and theoretical methods of mass determination are readily available. Pinheiro et al. (2014) compared the mass estimates resulting from four methods: (1) direct stellar-mass determinations from the objects’ spectra; (2) application of the empirical relation between stellar mass, effective temperature (T_{eff}), surface gravity ($\log g$), and metal abundance; (3) application of the empirical mass–luminosity relation; and (4) a comparison of the objects’ positions in the CMD with Padova isochrones. They found that their results from application of all four methods were comparable.

In this paper, we will use methods (2) and (3) to estimate the masses of the W UMa systems’ primary stars. In the context of method (2), M_1 is a function of $f(\log T_1, \log g, [\text{Fe}/\text{H}])$. The best-fitting results were derived by Torres et al. (2010); the resulting uncertainty in stellar mass is $\Delta \log(m_1/M_\odot) \simeq 0.027$ for $m_1 = 0.6M_\odot$. T_1 is subsequently estimated from the empirical relationship, and $\log g$ can be obtained from the best-fitting isochrone. Finally, for NGC 188 we adopt $[\text{Fe}/\text{H}] = -0.03$ dex (Dias et al. 2002). As regards method (3), the primary stellar mass can be calculated from the absolute magnitude of the W UMas (Henry & McCarthy 2015), while the absolute magnitude can be estimated from the relevant PL relation (see Section 4.2). The resulting root-mean-square of the fit is 0.032 in $\log(m_1/M_\odot)$. In Fig. 5, the difference between the two results is smaller than the statistical error (cf. Pinheiro et al. 2014) except for V_5 (V371 Cep; for a discussion, see Section 4). The primary stellar mass is not sensitive to the method used, so we use the masses from Torres et al. (2010) to determine the distances to our W UMas.

W UMas are overcontact binary systems. The primary star’s mass exceeds its luminosity, with the excess energy being transferred to its companion. The correction in mass required from a main-sequence star to the primary star of a W UMa system is given by $\Delta \log(m/M_\odot) = \frac{1}{4.4} \log(1 + U)$, where U is the fraction of energy of the primary star transferred to the secondary star (Mochnacki 1981). This correction is needed to compare the masses of main-sequence stars in detached binaries and of primary stars in W UMas: see Fig. 6.

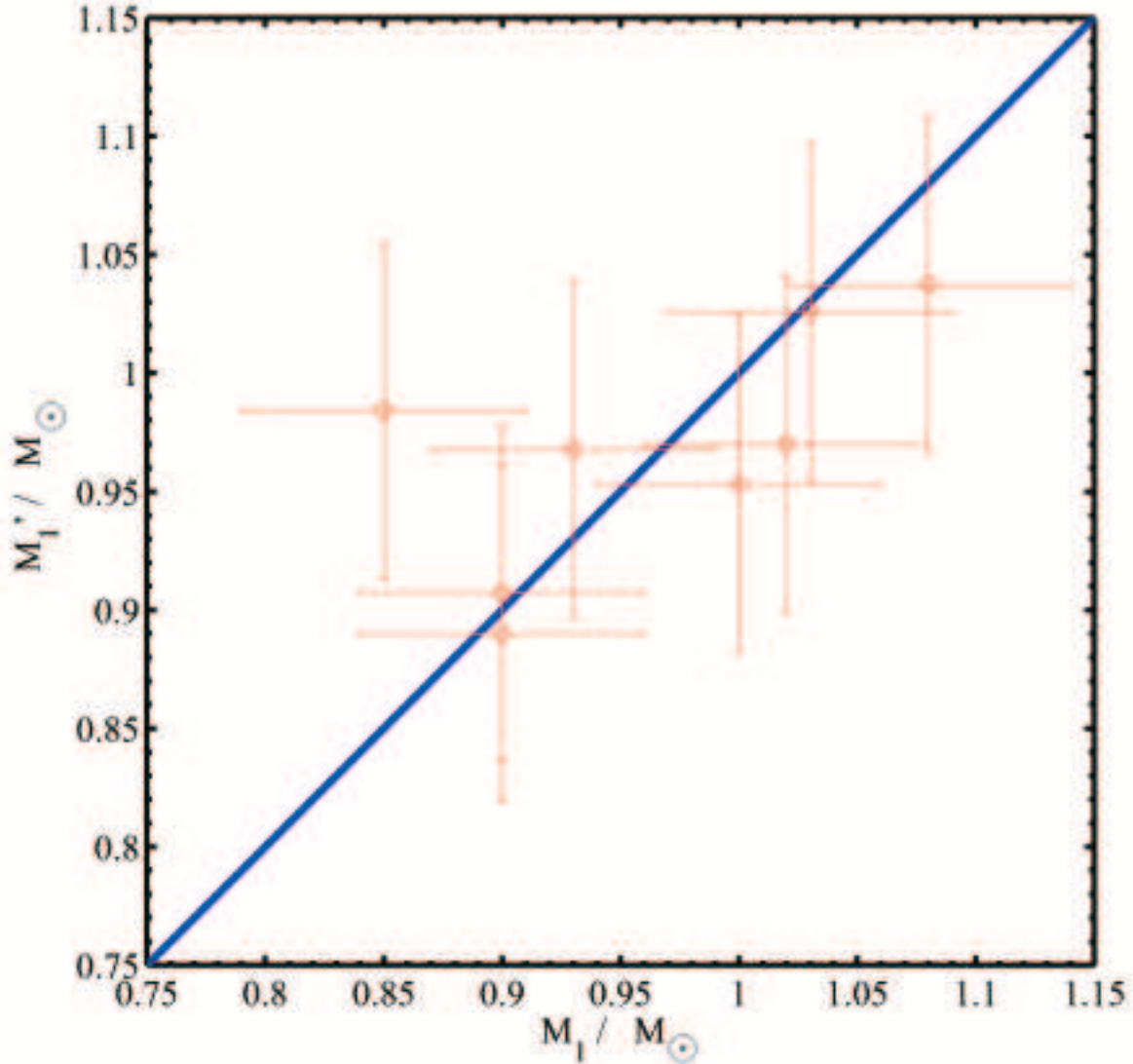


Fig. 5.— Comparison of primary stellar masses based on two different methods. The subscripts refer to the methods adopted. M_1 is estimated from the empirical relationship of Torres et al. (2010), while M'_1 is estimated from the empirical mass–luminosity relation (Henry & McCarthy 2015). Considering the prevailing error bars, most mass determinations are in agreement, except for V₅ (V371 Cep).

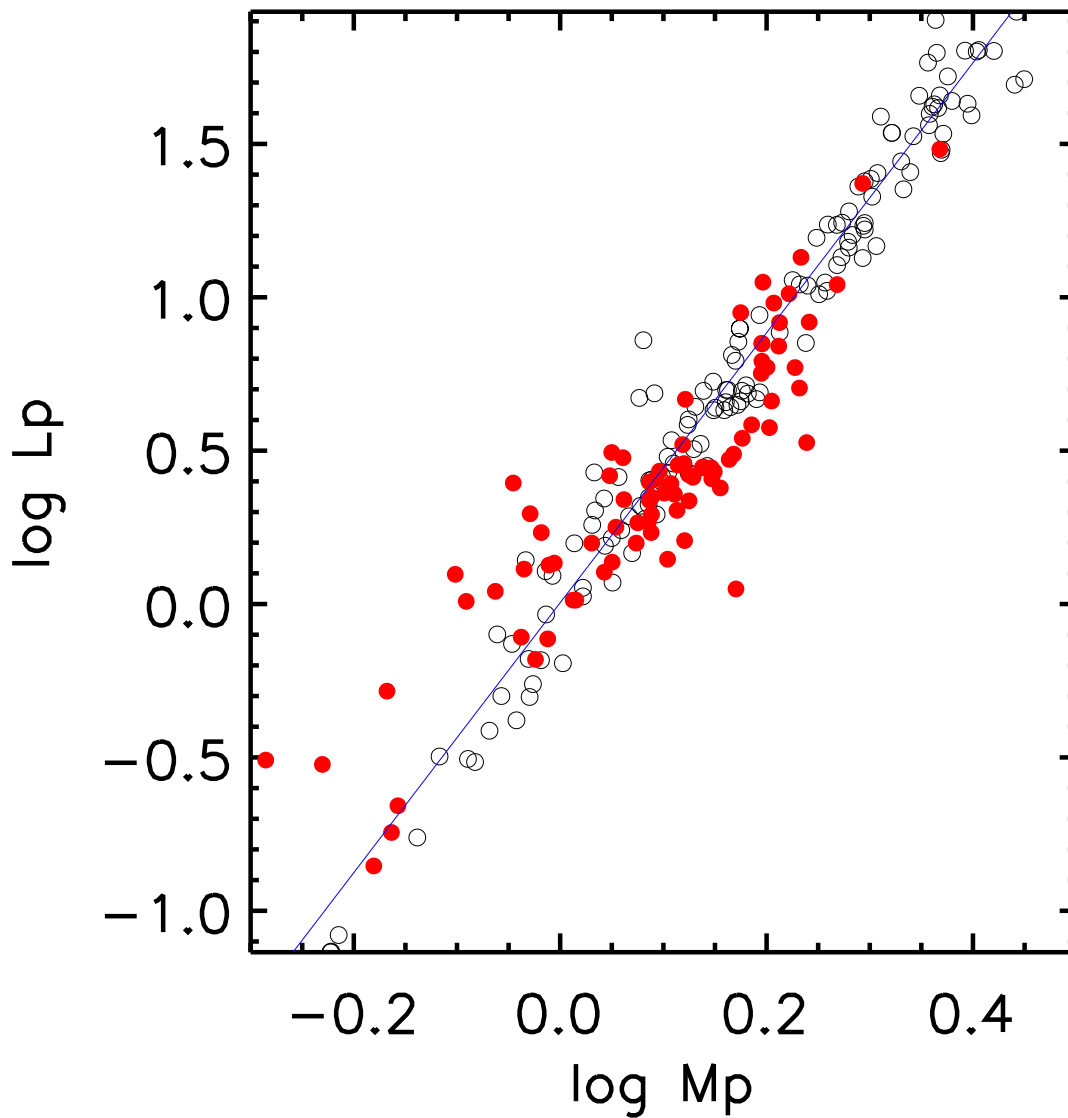


Fig. 6.— Open circles are 190 main-sequence stars in 95 detached binaries with mass and radius accuracies within $\pm 3\%$ (Torres et al. 2010). The solid bullets are the best-studied 100 W UMas of Yıldız & Doğan (2013). The masses of the solid bullets have been corrected onto the main-sequence scale as discussed in the text. The solid line represents the $L \propto M^{4.4}$ mass–luminosity relation for main-sequence stars. The corrected primary stellar masses of the W UMas are well fitted.

3.4. Distance determination

van Hamme & Wilson (1985) provided a method to estimate the absolute stellar mass from the observed parallax. Once the distance and luminosity are known sufficiently well, a suitable temperature indicator—such as the $(B - V)$ color—can permit calculation of a star’s absolute radius, R , by application of Stefan’s Law. In the Roche model for binary systems, the semi-major axis, a , is related to the size of the lobe-filling component. The mass ratio can be estimated from the light-curve solution even if the radial velocity has not been measured. Both parameters are needed in the application of Kepler’s Third Law to determine the absolute stellar mass, which in turn allows a distance determination.

Branly et al. (1996) derived an equation to estimate the distance based on q and the relative radius of the primary star, $r_1 = R_1/a$. They used the maximum V magnitude, V_{\max} , which is a superposition of the brightnesses of both component stars. They used L_1 for comparison with V_{\max} . Following their method, we use the combination of $L_1 + L_2$ instead of L_1 alone. From the fundamental equations

$$\begin{aligned} G(m_1 + m_2) &= (2\pi/P)^2 a^3; \\ a &= (R/R_\odot)/r; \\ L/L_\odot &= (T_{\text{eff}}/T_{\text{eff},\odot})^4 (R/R_\odot)^2; \\ M_{\text{bol}} &= M_V + \text{BC}, \end{aligned} \tag{2}$$

we can derive the distance modulus:

$$\begin{aligned} V_{\max} - M_V &= -39.189 + V_{\max} + \text{BC} + 10 \log T_1 + 5 \log r \\ &+ \frac{5}{3} \log m_1 + \frac{10}{3} \log P + \frac{5}{3} \log(1 + q); \\ r &= \left(r_1^2 + r_2^2 \left(\frac{T_2}{T_1} \right)^4 \right)^{\frac{1}{2}}. \end{aligned} \tag{3}$$

Here, G is the usual gravitational constant, M_V is the absolute V -band magnitude, M_{bol} is the bolometric luminosity and BC is the bolometric correction; r is the equivalent relative radius, which is a combination of r_1 and r_2 , and m_1 is expressed in units of M_\odot . The feasibility of using this method depends almost entirely on knowing the properties of the binary systems themselves; only the color excess is obtained from fitting the host OC’s isochrones to the observed cluster CMD features. Since the OC’s distance depends only very weakly on its color excess, this method is, in essence, an independent approach to determine the distances to the W UMa systems. Table 2 includes, for all stars, the parameters that result in the smallest residuals, which in turn can be used to derive their distances.

To estimate the expected uncertainties pertaining to the resulting distance modulus, we use

$$\begin{aligned} \sigma_{V-M_V}^2 = & \sigma_V^2 + \left(\frac{\partial \text{BC}}{\partial(V-R)} + 10 \frac{\partial \log T_{\text{eff}}}{\partial(V-R)} \right)^2 \sigma_{V-R}^2 + \\ & \left(\frac{5}{\ln 10} \frac{1}{r} \right)^2 \sigma_r^2 + \left(\frac{5}{3} \sigma_{\log M_1} \right)^2 + \left(\frac{10}{3 \ln 10} \frac{1}{P} \right)^2 \sigma_P^2 + \\ & \left(\frac{5}{3 \ln 10} \frac{1}{1+q} \right)^2 \sigma_q^2 + \left(\frac{5}{3 \ln 10} \right)^2 \frac{6}{r(1+q)} \eta_{rq} \sigma_r \sigma_q, \end{aligned} \quad (4)$$

where σ_q , σ_r , and σ_P are the uncertainties in the mass ratio, equivalent relative radius, and orbital period, respectively; η_{rq} is the correlation coefficient of r and q . In this equation, σ_V includes the photometric error (0.03–0.06 mag, depending on the filter considered), the uncertainty in our determination of the maximum magnitude (0.002–0.004 mag), as well as that in our extinction estimate (0.01 mag); σ_{V-R} encompasses the photometric error as well as the uncertainty in the reddening correction (0.002 mag). Since $(V-R)$ is estimated based on the average value of hundreds of data points, the statistical uncertainty is negligible, at only 0.0001–0.0002 mag. An uncertainty of $\sigma_{V-R} = 0.022$ –0.042 mag corresponds to an error of $\sigma_{T_1} = 100$ –200 K in our calculation.

The (partial) derivative of BC (and $\log T_{\text{eff}}$) to $(V-R)$, i.e., $\left(\frac{\partial \text{BC}}{\partial(V-R)} \right)$, can be estimated from interpolation of the equation, and σ_{m_1} can be derived from Torres et al. (2010). If the orbital solution is good enough, σ_V and σ_{V-R} represent the dominant components of σ_{V-M_V} . A prominent error in the orbital parameters, e.g., in P , q , or T_2 , will increase the corresponding error. The uncertainties affecting our estimates are all listed in Table 3. The maximum error is approximately 0.3 mag, although uncertainties of 0.1–0.2 mag are expected more commonly. We thus conclude that W UMa systems can be used to determine (individual) distances with an accuracy of (often significantly) better than 0.2 mag in distance modulus, provided that we have access to high-quality photometry and perform a careful and detailed analysis.

4. Discussion

4.1. Individual W UMa systems

Most previously publications treat V_3 (ER Cep) as a cluster member. This may be owing to the relatively small cluster distance moduli which were commonly measured prior to 1990 (e.g., Eggen & Sandage 1969; vandenBerg 1985) or because of a lack of proper-motion and radial-velocity data. Worden et al. (1978) determined an inclination of $i = 79^\circ \pm 3^\circ$ and

a mass ratio $q = 0.55 \pm 0.20$. They also estimated a distance modulus of $(m - M)_V^0 = 10.70 \pm 0.04$ mag, assuming $m_1 = 1.0M_\odot$, and attempted to use ER Cep to study the evolution of NGC 188. These authors point out that ER Cep is located just below the Hertzsprung gap in the CMD, so that the system could potentially be used to assess the validity of theories attempting to explain the relevant gap physics, provided that one’s mass accuracy is sufficient. Our results, $q = 0.62 \pm 0.01$ and $(m - M)_V^0 = 10.78 \pm 0.09$ mag, are in agreement with those of Worden et al. (1978). However, ER Cep’s proper motion, $(\mu_\alpha, \mu_\delta) = (-3.25 \pm 0.19, -0.98 \pm 0.19)$ mas yr⁻¹, deviates more than 3σ from the cluster’s mean proper motion, $(\mu_\alpha, \mu_\delta) = (-5.2 \pm 0.6, -0.3 \pm 0.6)$ mas yr⁻¹, which means that its cluster membership is questionable. Its distance modulus, $(m - M)_V^0 = 10.78 \pm 0.09$ mag is clearly significantly different from that of the cluster as a whole, $(m - M)_V^0 = 11.279 \pm 0.010$ mag (Hills et al. 2015).

A detailed check of its light curve shows that V_5 (V371 Cep) may not be a genuine W UMa system, since it exhibits clearly unequal minima and maxima, as well as a strange color and an unusual period. Its color is obviously redder than those of the other W UMas, which results in a lower color-based mass than its true mass: see Fig. 5. The apparent 0.2 mag difference between the primary and secondary minima implies that this object behaves more like an EB. Kaluzny & Shara (1987) also identified an EB-type light curve for this object, with a similar difference between the primary and secondary minima (Kaluzny 1990). Rucinski & Duerbeck (1997) treated V371 Cep as a poor thermal-contact or semidetached system and pointed out that this star is approximately 0.8 mag fainter than expected based on the PLC relation for W UMas. Liu et al. (2011) did not identify the unequal minima in their light curves, which may be owing to calibration problems affecting their three nights of observations. To obtain a good fit and following the commonly adopted approach, we added one spot to both the primary and secondary stars (see Table 2). We thus derived a distance

Table 3: Individual uncertainties (in mag) contributing to the total error in the distance modulus.

ID	σ	σ_V	$\sigma_{(V-R)}$	$\sigma_{\log m_1}$	σ_P	σ_r	σ_q	σ_{\max}
EP Cep	0.12	0.04	0.08	0.04	0.006	0.02	0.02	0.25
EQ Cep	0.11	0.04	0.08	0.04	0.005	0.02	0.02	0.23
ER Cep	0.09	0.03	0.06	0.04	0.004	0.02	0.02	0.20
ES Cep	0.09	0.03	0.06	0.04	0.004	0.02	0.02	0.20
V370 Cep	0.12	0.03	0.06	0.04	0.004	0.04	0.08	0.26
V369 Cep	0.10	0.03	0.06	0.04	0.004	0.04	0.02	0.20
V371 Cep	0.10	0.03	0.06	0.04	0.004	0.05	0.05	0.22
V782 Cep	0.12	0.03	0.06	0.04	0.004	0.04	0.07	0.25

modulus of $(m - M)_V^0 = 11.56 \pm 0.10$ mag, which deviates from the distance obtained from the other W UMas. This thus shows that V371 Cep is not a well-behaved W UMa-type cluster member.

The orbital-parameter solutions for EQ Cep and ER Cep are comparable to those determined by Liu et al. (2011). Our ES Cep and EP Cep results are also comparable with literature determinations, particularly with those of Zhu et al. (2014), considering that the systematic uncertainty in the mass ratio is approximately $\Delta q_{\text{sys}} = 0.1\text{--}0.2$ in the absence of any radial-velocity information. For V369 Cep, we obtain a larger $q = 1.90$, which is in accordance with Branly et al. (1996). In fact, in their $\Sigma - q$ diagram, Σ does not show any difference for $q \in [0.6, 2.0]$. We find that $q = 1.90$ is only 0.5% better than other q values in this range. Branly et al. (1996) obtained similar results for their five W UMas (EP Cep, ER Cep, EQ Cep, ES Cep, and V369 Cep) as we do, despite the differences in our approaches.

The orbital parameters of V370 Cep and V782 Cep have been determined for the first time here. Since both exhibit small amplitudes of around 0.1 mag, high-accuracy observations are needed to obtain obvious W UMa-type light curves. We therefore selected all data points with photometric errors of less than 0.02 mag for our light-curve fitting. From Fig. 4 it follows that our light-curve fit closely matches the theoretical curve.

4.2. The distance to NGC 188

NGC 188 is a well-studied Galactic open cluster, and as such its distance has been measured by many authors. Small cluster distance moduli of around $(m - M)_V^0 = 10.80$ mag were commonly measured prior to 1990 (e.g., Eggen & Sandage 1969; vandenBerg 1985). Branly et al. (1996) derived two different distance moduli, $(m - M)_V^0 = 10.80$ mag and $(m - M)_V^0 = 11.40$ mag, based on 5 W UMas. During the last decade, a larger value for the cluster’s distance modulus has increasingly been preferred. vandenBerg & Stetson (2004) derived $(m - M)_V$ values of 11.22–11.54 mag for NGC 188, depending on the chemical composition assumed. Meibom et al. (2009) determined a distance modulus of $(m - M)_V^0 = 11.24 \pm 0.09$ mag based on a single EA-type eclipsing binary system (EA-type systems are detached or semi-detached binary systems whose secondary minima are almost non-existent). Recently, Hills et al. (2015) published a detailed analysis of the isochrone-fitting method to determine the distance to NGC 188. They obtained an accurate average distance of $(m - M)_V^0 = 11.279 \pm 0.010$ mag and $(m - M)_V^0 = 11.289 \pm 0.008$ mag based on observations in 15 filters and for two different isochrone models. Although their statistical uncertainty is small, the corresponding systematic error would be 0.05–0.10 mag, which is mainly driven by lingering uncertainties in both the reddening and the theoretical models. In this paper, we

derived a distance modulus of $(m - M)_V^0 = 11.35 \pm 0.10$ mag from isochrone fitting, which is indeed comparable to previous determinations. We also and independently obtained a distance modulus of $(m - M)_V^0 = 11.35 \pm 0.12$ mag based on a combined analysis of seven of the eight W UMas in our sample, not including the foreground object V_3 .

Having carefully considered all uncertainties associated with this approach, we have thus obtained a distance estimate that is indeed somewhat better than the distances resulting from the empirical, formulaic approach of Rucinski (1994). Considering all these results from independent methods, we support a robust distance determination to NGC 188 of 1800 ± 80 pc. The distance error associated with the W UMa method is comparable with that from isochrone fitting. NGC 188 is a well-studied cluster, so that the precision of the isochrone-fitting method is assured. Unfortunately, fewer than half of the OCs in the DAML02 OC catalog (Dias et al. 2002) are suitable for use with the isochrone-fitting method because of the lack of a prominent main sequence, in addition to an absence of radial-velocity and proper-motion data. The W UMa method further developed here can play an important role in determining distances to these clusters.

The W UMa method does not depend on a cluster’s age, so it can provide constraints to estimates of the cluster age. Clusters can provide useful clues regarding the formation of W UMas. Although W UMa systems are very common in stellar populations, their formation mechanism is still controversial. One possible formation scenario is that they form as a binary system from two close mass overdensities during the time of molecular-cloud collapse, before they reach the zero-age main sequence. In this case, the frequency of W UMas in the field and in OCs must be similar. An alternative scenario suggests that they are the result of evolved, detached stars. In this latter scenario, the system’s orbital period becomes shorter over time because of angular momentum loss caused by magnetic braking (Schatzman 1962), which thus implies that the separation between both components decreases. The frequency of W UMas in clusters of different ages can provide clues as to their formation. In a region with a radius of 20 arcmin around the NGC 188 cluster center, the frequency of W UMas is of order 10 per 1000 stars, which is significantly higher than the average EB-type binary frequency of about 4 per 1000 stars (Rucinski 1994) or that of EA-type binaries of about 2 per 1000 stars. Consequently, it seems that W UMas may indeed be capable of surviving to intermediate ages of several billion years and thus that they are more likely the products of the evolution of detached stars. This suggestion should be confirmed by studying a large sample of OC W UMas.

4.3. Comparison with the W UMa PLC Relation

Rucinski (1994) pointed out that W UMa-type binaries follow a strict (empirical) PLC relationship, $M_V = -4.30 \log P + 3.28(B-V)_0 + 0.04 \text{ mag}$ ($\sigma = 0.17 \text{ mag}$). This relationship is simple and suitable for application to most W UMa systems. However, it has been established in part based on 5 W UMa systems in NGC 188. Therefore, distances derived based on this PLC relation are not independent for NGC 188. Here we provide a distance comparison using the light-curve solutions. Table 4 shows the two distances, while for the PLC relation we adopt the same color and period as used for the determination of the light-curve solution distance. Both distances are in good mutual agreement. For the average distance, the light-curve solution distance seems slightly better. This may be owing to the influence of the mass ratio, q , which is not included in the construction of the PLC relation but it is considered in the context of the light-curve solution distance. Rucinski & Duerbeck (1997) evaluated the influence of q and found that it has a $\sigma = 0.06 \text{ mag}$ effect on the PLC relation’s zero point. However, more open cluster W UMas with homogeneous photometry are needed to draw stronger conclusions. In addition, the good agreement of the two distance measures implies that we can, in principle, constrain the coefficients of the empirical PLC relation more tightly.

4.4. Berkeley 39

Berkeley 39 is a similar OC to NGC 188. It contains 11 W UMa systems (Kaluzny et al. 1993; Mazur et al. 1999). Consequently, this cluster and its W UMa sample can be used to double check the applicability of W UMa distance estimation. Kiron et al. (2011) derived the orbital solutions for seven W UMas in Berkeley 39. Among these seven W UMas, V_6, V_7, V_8 , and V_{10} are main-sequence W UMas, while the remaining three stars are blue straggler-type W UMas. For the four main-sequence W UMas, we determine a distance modulus $(m - M)_V^0 = 13.09 \pm 0.23 \text{ mag}$, considering a reddening of $E(B - V) = 0.17 \text{ mag}$ and a metallicity $[\text{Fe}/\text{H}] = -0.2 \text{ dex}$ (Bragaglia et al. 2012). This distance modulus is comparable to previous estimates, i.e., $(m - M)_V^0 = 12.94 \pm 0.26 \text{ mag}$ (Bragaglia et al. 2012), $(m - M)_V^0 = 13.11 \pm 0.31 \text{ mag}$ (Kaluzny & Richtler 1989; Mazur et al. 1999), and $(m - M)_V^0 = 13.20 \pm 0.21 \text{ mag}$ (Carraro et al. 1994), considering differences in the adopted reddening corrections. Compared with the results for NGC 188, the uncertainty in the distance is somewhat larger because Berkeley 39 is 3 mag fainter, which increases the errors in both V_{max} and T_1 .

4.5. Period–luminosity relation

Rucinski (2006) published a simple $M_V = M_V(\log P)$ calibration, $M_V = (-1.5 \pm 0.8) - (12.0 \pm 2.0) \log P$, $\sigma = 0.29$ mag, for 21 W UMa systems with good *Hipparcos* parallaxes and All Sky Automated Survey (ASAS) V -band maximum magnitudes.² We therefore established the equivalent relationship using our V -band data, combined with the independently determined OC distance and extinction. We estimated a maximum absolute magnitude for each W UMa based on distance from Hills et al. (2015), $(m - M)_V^0 = 11.28$ mag, and reddening, $E(V - R) = 0.062$ mag. The results are shown in Table 5 and Fig. 7. We also added the four W UMas in Berkeley 39, for comparison, using $(m - M)_V^0 = 12.94$ mag, $E(B - V) = 0.17$ mag, and $[\text{Fe}/\text{H}] = -0.2$ dex (Bragaglia et al. 2012). For large samples of W UMas, we expect a flat PL relation. This will be discussed in a subsequent paper, once we have collected sufficiently large numbers of W UMas spanning a suitably large range in $\log P$.

4.6. Physical parameters of our sample W UMas

The distance modulus to NGC 188 we have determined here matches the current best estimate, $(m - M)_V^0 = 11.28$ mag (Hills et al. 2015) very well. If we now adopt this latter distance modulus, we can in turn derive the luminosities, masses, and radii of the W UMa systems that are confirmed NGC 188 cluster members. For the foreground W UMa system V3, a distance modulus of $(m - M)_V^0 = 10.70$ mag is adopted. The luminosities can be estimated from the systems’ apparent magnitudes, combined with the adopted distance modulus, reliable extinction values, and a proper bolometric correction. The radii R_1, R_2 can then be derived from their effective temperatures, which are known. Since W UMa stars satisfy a mass–radius relation, with some corrections M_1 follows directly. For simplicity, we can straightforwardly adjust the semi-major axis, a (i.e., varying only one parameter) in the W–D LC code to match the theoretical to the observed luminosity. The corresponding R_1, R_2, M_1 , and M_2 for this optimally chosen a are the resulting masses and radii for the W UMa systems.

The final physical parameters thus derived are included in Table 6. Based on these

²In Eq. (3), the luminosity of the W UMa systems is a function of $f(T_{\text{eff}}, P, q, M, r)$, while their masses and radii are known to correlate with T_{eff} (Rucinski 1994). In principle, the luminosity of W UMas is determined by their intrinsic colors, orbital periods, and mass ratios. Since for most W UMas we only have access to their orbital periods, it is indeed meaningful to establish a simple PL relation to estimate approximate distances.

Table 4: Comparison of distance moduli based on the two different methods employed in this paper.

ID	$(m - M)_V^0$ (This work) (mag)	$(m - M)_V^0$ (PLC) (mag)
EP Cep	11.382 ± 0.117	11.502
EQ Cep	11.280 ± 0.111	11.383
ER Cep	10.781 ± 0.093	10.744
ES Cep	11.188 ± 0.092	11.153
V370 Cep	11.299 ± 0.122	11.341
V369 Cep	11.412 ± 0.095	11.425
V371 Cep	11.563 ± 0.101	11.837
V782 Cep	11.314 ± 0.115	11.356
Average (except V_3 and V_5)	11.313 ± 0.079	11.360 ± 0.117
Average (except V_3)	11.348 ± 0.119	11.428 ± 0.210

Table 5: Periods and maximum absolute magnitudes for six W UMas.

ID	V_{\max} (mag)	P (d)	M_V (mag)	σ_{M_V} (mag)
EP Cep	16.670	0.2897446	5.144	0.25
EQ Cep	16.549	0.3069522	5.023	0.23
ES Cep	15.729	0.3424570	4.203	0.20
V370 Cep	16.131	0.3304319	4.605	0.26
V369 Cep	16.146	0.3281916	4.620	0.20
V782 Cep	15.791	0.3581278	4.267	0.25

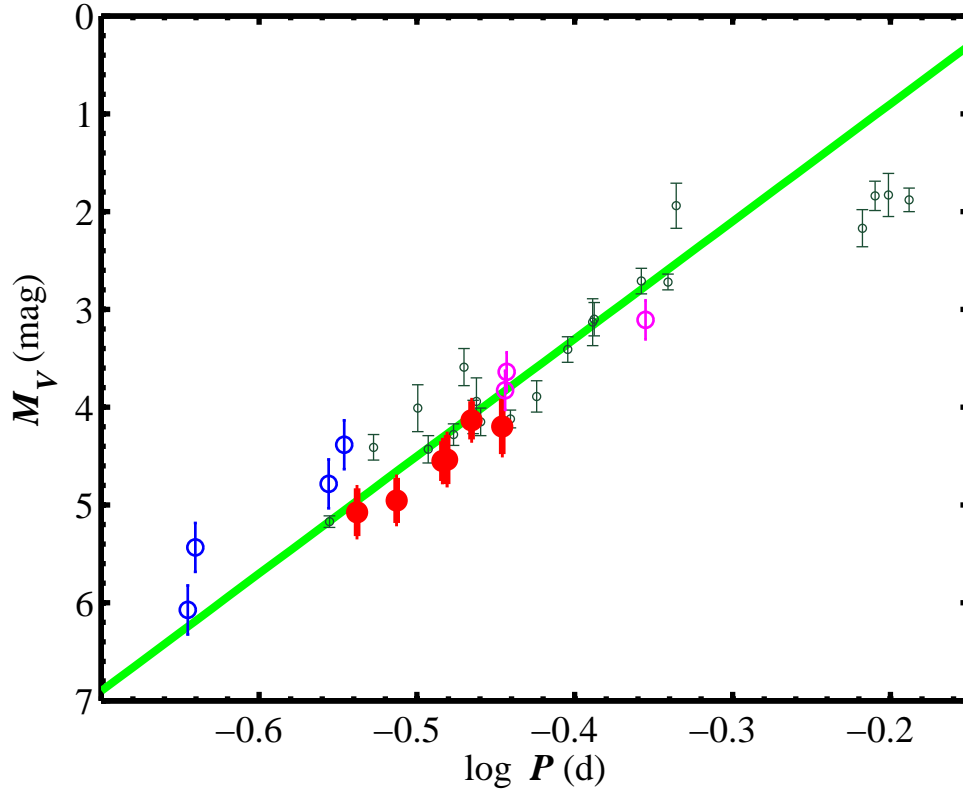


Fig. 7.— V -band W UMa PL relation. The heavy red dots are the six NGC 188 W UMas retained for our analysis, while the four blue circles are main-sequence W UMas in Berkeley 39. The magenta circles are three W UMas in M67. The green solid line is the PL relation for 21 W UMas (small black points with error bars) from Rucinski (2006).

parameters, V371 Cep is likely a subgiant or semi-detached contact binary. EP Cep, EQ Cep, V369 Cep, and V782 Cep are obviously W-type W UMa systems, since their less massive component stars have higher temperatures. ER Cep and V370 Cep are more likely W-type than A-type W UMa systems, because their temperatures are lower than those typical of most A-type W UMa systems. It is hard to classify ES Cep. We have estimated the initial masses based on the method of Yıldız & Doğan (2013). Following the criteria proposed by the latter authors, A-type W UMa systems have $M_{1i} > 1.8M_{\odot}$, while W-type W UMa systems are characterized by $M_{1i} < 1.8M_{\odot}$. We obtained the same classifications for these W UMa systems (see Table 7). Yıldız (2014) proposed a method to derive the ages of W UMa systems based on their initial masses and the current masses derived on the basis of the mass–luminosity relation pertaining to the secondary components. We also calculated the ages of our seven sample W UMa systems. We found these values to be in accordance with the overall age of NGC 188 (5–6 Gyr, Hills et al. 2015)), except for ER Cep, which is a foreground W UMa system.

Since we have adopted more accurate distance, better photometric calibrations, and because we have combined different methods to derive the masses, our mass determination for each W UMa system is more accurate than previously published values. Liu et al. (2011) obtained $M_1 = 0.97M_{\odot}$ and $M_2 = 0.51M_{\odot}$ for EQ Cep, which is comparable to our mass. However, they used the distance to NGC 188 in order to calculate the mass of the foreground system ER Cep. As a consequence, their derived values, $M_1 = 2.42M_{\odot}$ and $M_2 = 1.09M_{\odot}$, are unrealistic for a W UMa system with a temperature around 5000 K. Zhu et al. (2014) obtained primary masses, M_1 , of around $0.75 M_{\odot}$ for three W UMa systems, i.e., EP Cep, ES Cep, and V369 Cep. These values are underestimates. The corresponding ages of these W UMa systems, based on these underestimated masses, are close to a Hubble time, which is not in agreement with the cluster age.

Table 6: Physical parameters of our eight sample W UMa systems.

ID	M_1 (M_{\odot})	M_2 (M_{\odot})	R_1 (R_{\odot})	R_2 (R_{\odot})	a (R_{\odot})	L_1 (L_{\odot})	L_2 (L_{\odot})	T_1 (K)	T_2 (K)	P (days)
EP Cep	0.90 ± 0.03	0.17 ± 0.02	1.01 ± 0.04	0.48 ± 0.03	1.88 ± 0.08	0.67 ± 0.03	0.22 ± 0.10	5074 ± 177	5600 ± 177	0.2897
EQ Cep	0.90 ± 0.03	0.43 ± 0.02	0.95 ± 0.06	0.68 ± 0.05	2.10 ± 0.12	0.62 ± 0.05	0.40 ± 0.09	4975 ± 169	5275 ± 169	0.3070
ER Cep	1.00 ± 0.02	0.63 ± 0.02	0.91 ± 0.03	0.74 ± 0.03	2.14 ± 0.07	0.80 ± 0.05	0.48 ± 0.08	5505 ± 135	5383 ± 135	0.2857
ES Cep	1.08 ± 0.02	0.85 ± 0.02	1.02 ± 0.08	0.91 ± 0.07	2.56 ± 0.20	1.21 ± 0.06	0.79 ± 0.13	5582 ± 139	5308 ± 139	0.3425
V371 Cep	0.85 ± 0.03	0.80 ± 0.03	1.38 ± 0.04	1.35 ± 0.03	3.48 ± 0.12	0.95 ± 0.10	0.79 ± 0.12	4935 ± 153	4780 ± 153	0.5860
V370 Cep	1.02 ± 0.03	0.53 ± 0.03	0.96 ± 0.08	0.82 ± 0.07	2.32 ± 0.18	0.97 ± 0.07	0.45 ± 0.15	5383 ± 213	5175 ± 213	0.3304
V369 Cep	0.93 ± 0.02	0.49 ± 0.02	1.01 ± 0.08	0.76 ± 0.07	2.25 ± 0.17	0.77 ± 0.06	0.61 ± 0.08	5088 ± 137	5546 ± 137	0.3282
V782 Cep	1.03 ± 0.03	0.64 ± 0.03	1.05 ± 0.07	0.84 ± 0.06	2.51 ± 0.17	1.06 ± 0.11	0.89 ± 0.15	5370 ± 189	5750 ± 189	0.3581

5. Conclusions

Observations of the old OC NGC 188 were obtained with the recently commissioned 50BiN telescope in V and R . We collected 36 nights of time-series data, spanning an unprecedented total of 3000 frames for each star. To select genuine cluster members, we performed a detailed radial-velocity and proper-motion analysis. The radial velocity of NGC 188 is $v_{\text{RV}} = -42.32 \pm 0.90 \text{ km s}^{-1}$, while its proper motion is $(\mu_\alpha, \mu_\delta) = (-5.2 \pm 0.6, -0.3 \pm 0.6) \text{ mas yr}^{-1}$. Of our total sample of 914 stars, 532 stars are probable cluster members. They delineate an obvious cluster sequence down to $V = 18 \text{ mag}$. We use the Dartmouth stellar evolutionary isochrones (Dotter et al. 2008) to match the cluster members, adopting an age of 6 Gyr and solar metallicity. A distance modulus and reddening of, respectively, $(m - M)_V^0 = 11.35 \pm 0.10 \text{ mag}$ and $E(V - R) = 0.062 \pm 0.002 \text{ mag}$ were obtained.

Accurate light-curve solutions were obtained for the eight W UMas, and parameters such as their mass ratios and the components’ relative radii were estimated. We subsequently estimated the distance moduli for the W UMas, independent of the cluster distance. W UMas can be used to derive distance moduli with an accuracy of often significantly better than 0.2 mag. Object V_5 (V371 Cep) is not a genuine W UMa system. V_3 (ER Cep) was excluded from the distance-modulus analysis because of its low cluster-membership probability. For the remaining six OC W UMas—EP Cep, EQ Cep, ES Cep, V369 Cep, V370 Cep, and V782 Cep—we obtained a joint best-fitting distance modulus of $(m - M)_V^0 = 11.31 \pm 0.12 \text{ mag}$, which is comparable to the result from our isochrone fits, as well as with previous results from the literature. The resulting accuracy is better than that resulting from application of the previously established empirical parametric approximation.

To double check our results for NGC 188 and the applicability of W UMas as distance tracer, we applied it to the OC Berkeley 39. Based on four of its W UMas, we derived a

Table 7: Initial masses and ages of our seven sample W UMa systems.

ID	M_{2i} (M_\odot)	M_{1i} (M_\odot)	t (Gyr)	Type
EP Cep	1.56 ± 0.06	0.43 ± 0.02	6.9 ± 1.2	W
EQ Cep	1.42 ± 0.08	0.56 ± 0.03	7.4 ± 1.6	W
ER Cep	1.07 ± 0.11	0.85 ± 0.09	12.8 ± 4.2	W
ES Cep	1.76 ± 0.18	0.65 ± 0.07	5.3 ± 2.8	A(W)
V370 Cep	1.29 ± 0.18	0.76 ± 0.11	8.8 ± 3.7	W
V369 Cep	1.52 ± 0.10	0.59 ± 0.03	5.6 ± 1.3	W
V782 Cep	1.46 ± 0.16	0.75 ± 0.08	5.5 ± 1.9	W

distance modulus of $(m-M)_V^0 = 13.09 \pm 0.23$ mag, which is also in accordance with literature results. W UMas as distance tracers have significant advantages for poorly studied clusters. The six W UMas in NGC 188 satisfy a tight PL relation. Armed with the latter, W UMas could indeed play an important role in measuring distances and to map Galactic structures on more ambitious scales than done to date.

Based on better distances and photometry, more accurate physical parameters for eight W UMa systems were derived. Using the evolutionary W UMa model of Yıldız & Doğan (2013), the initial masses of seven W UMa systems were estimated. All seven W UMa systems have initial primary masses below $1.8 M_\odot$, which means that they have evolved along the evolutionar W-type route (i.e., through angular-momentum evolution within a convective envelope). The ages of seven sample W UMa systems were estimated based on their initial masses and the current luminosity-based masses of the secondary components. Six of our cluster W UMa systems have similar ages as the host cluster itself, which provides confirmation of the age-dating method of Yıldız (2014).

We are grateful for research support from the National Natural Science Foundation of China through grants 11373010 and 11473037.

REFERENCES

- An, D., Terndrup, D. M., & Pinsonneault, M. H. 2007, *ApJ*, 671, 1640
- Bragaglia, A., Gratton, R. G., Carretta, E., et al. 2012, *A&A*, 548, 122
- Branly, R. M., Athauda, R. I., Fillingim, M. O., & van Hamme, W. 1996, *Ap&SS*, 235, 149
- Buser, R., & Kurucz, R. L. 1992, *A&A*, 264, 557
- Carraro, G., Chiosi, C., Bressan, A., & Bertelli, G. 1994, *A&AS*, 103, 375
- Chen, X. D., de Grijs, R., & Deng, L. C. 2015, *MNRAS*, 446, 1268
- Deng, L. C., Xin, Y., Zhang, X. B., et al. 2013, in: *IAU Symp. 288, Astrophysics from Antarctica*, ed. T. Montmerle et al. (Cambridge: Cambridge Univ. Press), 318
- Dias, W. S., Alessi, B. S., Moitinho, A., & Lépine, J. R. D. 2002, *A&A*, 389, 871
- Dotter, A., Chaboyer, B., Jevremovic, D., et al. 2008, *ApJS*, 178, 89
- Duerbeck, H. W. 1984, *Ap&SS*, 99, 363

- Eggen, O. J., & Sandage, A. 1969, *AJ*, 158, 669
- Geller, A. M., Mathieu, R. D., Harris, H. C., & McClure, R. D. 2008, *AJ*, 135, 2264
- Geller, A. M., & Mathieu, R. D. 2012, *AJ*, 144, 54
- Girardi, L., Bressan, A., Bertelli, G., & Chiosi, C. 2000, *A&AS*, 141, 371
- Henry, T., & McCarthy, D. J. 1993, *AJ*, 106, 773
- Hilditch, R. W., King, D. J., McFarlane, T. M. 1988, *MNRAS*, 231, 341
- Hills, S., von Hippel, T., Courteau, S., & Geller, A. M. 2015, *AJ*, 149, 94
- Hoffmeister, C. 1964, *Inf. Bull. Var. Stars*, 67, 1
- Kaluzny, J. 1990, *AcA*, 40, 61
- Kaluzny, J., & Shara, M. M. 1987, *ApJ*, 314, 585
- Kaluzny, J., & Richtler, T. 1989, *AcA*, 39, 139
- Kaluzny, J., Mazur, B., & Krzeminski, W. 1993, *MNRAS*, 262, 49
- Kiron, Y. R., Sriram, K., & Vivekananda, R. P. 2011, *RAA*, 11, 1469
- Lejeune, Th., Cuisinier, F., Buser, R. 1997, *A&AS*, 125, 229
- Liu, L., Qian, S. B., et al. 2011, *MNRAS*, 415, 3006
- Mazur, B., Krzeminski, W., & Kaluzny, J. 1999, *AcA*, 49, 551
- Meibom, S., Grundahl, F., Clausen, J. V. et al., 2009, *AJ*, 137, 5086
- Mochnecki, S. W. 1981, *ApJ*, 245, 650
- Pinheiro, F. J. G., Fernandes, J. M., Cunha, M. S., et al. 2014, *MNRAS*, 445, 2223
- Platais, I., Kozhurina-Platais, V., Mathieu, R. D., Girard, T. M., & van Altena, W. F. 2003, *AJ*, 126, 2922
- Rucinski, S. M. 1994, *PASP*, 106, 462
- Rucinski, S. M., & Duerbeck, H. W. 1997, *PASP*, 109, 1340
- Rucinski, S. M. 2000, *AJ*, 120, 319

- Rucinski, S. M. 2001, *AJ*, 122, 1007
- Rucinski, S. M. 2006, *MNRAS*, 368, 1319
- Sandage, A., & Tammann, G. A. 2008, *ApJ*, 686, 779
- Sarajedini, A., von Hippel, T., Kozhurina-Platais, V., & Demarque, P. 1999, *AJ*, 118, 2894
- Schatzman, E. 1962, *AnAp*, 25, 18
- Torres, G., Andersen, J., & Giménez A. 2010, *A&A Rev.*, 18, 67
- vanden Berg, D. A. 1985, *ApJS*, 58, 711
- VandenBerg, D. A., & Stetson, P. B. 2004, *PASP*, 116, 997
- van Hamme, W., & Wilson, R. E. 1985, *Ap&SS*, 110, 169
- van Hamme, W. 1993, *AJ*, 106, 2096
- Wilson, R. E., & Devinney, E. J. 1971, *ApJ*, 166, 605
- Wilson, R. E. 1979, *ApJ*, 234, 1054
- Wilson, R. E. 1990, *ApJ*, 356, 613
- Worden, S. P., Coleman, G. D., Rucinski, S. M., & Whelan, J. A. J. 1978, *MNRAS*, 183, 33
- Yi, S., Demarque, P., Kim, Y. C., et al. 2001, *ApJS*, 136, 417
- Yıldız, M., & Doğan, T. 2013, *MNRAS*, 430, 2029
- Yıldız, M. 2014, *MNRAS*, 437, 185
- Zhang, X. B., Deng, L., Tian, B., & Zhou, X. 2002, *AJ*, 123, 1548
- Zhang, X. B., Deng, L. C., Zhou, X., & Xin, Y. 2004, *MNRAS*, 355, 1369
- Zhu, L. Y., Qian, S. B., Soonthornthum, B., et al. 2014, *AJ*, 147, 42